

---

# Reasoning to Edit: Hypothetical Instruction-Based Image Editing with Visual Reasoning

---

Qingdong He<sup>1\*</sup> Xueqin Chen<sup>2\*</sup> Chaoyi Wang<sup>3</sup> Yanjie Pan<sup>4</sup> Xiaobin Hu<sup>1</sup> Zhenye Gan<sup>1</sup>  
Yabiao Wang<sup>1</sup> Chengjie Wang<sup>1</sup> Xiangtai Li<sup>5</sup> Jiangning Zhang<sup>1</sup>

<sup>1</sup>YouTu Lab, Tencent <sup>2</sup>TU Delft <sup>3</sup>University of Chinese Academy of Sciences  
<sup>4</sup>Fudan University <sup>5</sup>Nanyang Technological University

## Abstract

Instruction-based image editing (IIE) has advanced rapidly with the success of diffusion models. However, existing efforts primarily focus on simple and explicit instructions to execute editing operations such as adding, deleting, moving, or swapping objects. They struggle to handle more complex implicit hypothetical instructions that require deeper reasoning to infer plausible visual changes and user intent. Additionally, current datasets provide limited support for training and evaluating reasoning-aware editing capabilities. Architecturally, these methods also lack mechanisms for fine-grained detail extraction that support such reasoning. To address these limitations, we propose **Reason50K**, a large-scale dataset specifically curated for training and evaluating hypothetical instruction-reasoning image editing, along with **ReasonBrain**, a novel framework designed to reason over and execute implicit hypothetical instructions across diverse scenarios. Reason50K includes over 50K samples spanning four key reasoning scenarios: Physical, Temporal, Causal, and Story reasoning. ReasonBrain leverages Multimodal Large Language Models (MLLMs) for editing guidance generation and a diffusion model for image synthesis, incorporating a Fine-grained Reasoning Cue Extraction (FRCE) module to capture detailed visual and textual semantics essential for supporting instruction reasoning. To mitigate the semantic loss, we further introduce a Cross-Modal Enhancer (CME) that enables rich interactions between the fine-grained cues and MLLM-derived features. Extensive experiments demonstrate that ReasonBrain consistently outperforms state-of-the-art baselines on reasoning scenarios while exhibiting strong zero-shot generalization to conventional IIE tasks. Our dataset and code will be released publicly at <https://github.com/hithqd/ReasonBrain>.

## 1 Introduction

The successful deployment of diffusion models [40, 12] in text-to-image (T2I) generation [33, 36, 37, 10] has significantly accelerated the development of *instruction-based image editing* (IIE) [31]. IIE focuses on performing precise and localized modifications on a source image in response to human commands, thereby enhancing the controllability and accessibility of visual manipulation [7]. Prior works typically utilize the CLIP-based text encoder inherent in T2I diffusion models for instruction embedding [5, 48, 18, 51, 8, 50], which is insufficient for comprehending complex instructions. To address this limitation, recent methods [42, 17, 30, 45, 23, 52, 41] have proposed substituting it with multimodal large language models (MLLMs) [43, 27], enabling richer cross-modal understanding

---

\*Equal contributions.



Figure 1: Current efforts fail to handle hypothetical instructions, producing incorrect results, while our method generates plausible, reasoning-aware edits.

and better alignment with user intent. However, despite the significant progress achieved by these efforts, the following limitations remain underexplored:

**(L1) Overlooking hypothetical instructions.** Existing IIE methods are primarily designed to handle simple, explicit, and goal-directed instructions (e.g., “remove the dog”), which typically correspond to straightforward editing operations such as adding, replacing, or deleting objects. However, users often begin without a clear editing objective and instead express ambiguous intent through hypothetical instructions (e.g., “What would happen if the ice cube was left in the sun?”). As illustrated in Fig. 1, current methods struggle to interpret and act on such inputs. Successfully addressing these cases requires models to go beyond surface-level edits and perform deeper reasoning about real-world context, physical changes, and the causal or temporal implications of the instruction. Moreover, currently there is no dataset specifically designed for hypothetical instruction-based editing that offers sufficient scale and scenario diversity [17, 46, 19, 29].

**(L2) Insufficient reasoning ability.** While integrating MLLMs [43, 27] can enhance instruction comprehension and improve alignment with user commands to some extent, these models still lack dedicated mechanisms for deep reasoning over hypothetical instructions (see Fig. 1 results of SmartEdit). We attribute this limitation to the prevailing paradigm’s reliance on coarse-grained features extracted directly from the input image and instruction, which fail to capture the fine-grained semantic cues necessary for implicit reasoning or fully exploit the MLLM’s embedded world knowledge [44]. For instance (Fig. 1(a)), reasoning over such an instruction requires jointly interpreting both visual and textual cues. Visually, elements like the cube’s sharp edges, surface gloss, and surrounding environment reveal its physical state and context. Textually, features such as conditional phrasing, object references, and temporal expressions together suggest a melting process.

To address these limitations, we propose a unified solution: a large-scale hypothetical instruction-based dataset, **Reason50K**, and a tailored reasoning-aware framework, **ReasonBrain**. Reason50K comprises diverse hypothetical instructions spanning four reasoning categories: physical, temporal, causal, and story-based reasoning, totaling 51,039 samples. Each sample consists of a source image, a hypothetical instruction, and a corresponding target image that reflects the intended edit. ReasonBrain consists of an MLLM and a diffusion model, augmented with two specialized modules for visual guidance, reasoning, and semantic enrichment: the Fine-grained Reasoning Cue Extraction (FRCE) module and the Cross-Modal Enhancer (CME). The FRCE module extracts detailed reasoning cues through two branches: the visual reasoning branch captures both local and global visual semantics to model spatial relationships and object-level interactions, while the textual reasoning branch identifies key object references and contextual intent from hypothetical instructions, enriched with relevant visual context. These fine-grained features, combined with multi-scale image tokens and textual embeddings, are input to the MLLM alongside learnable tokens to implicitly generate reasoning-aware visual guidance. Finally, the CME enhances these signals via semantic complementarity across modalities, producing well-aligned, semantically rich guidance for diffusion-based image editing. In sum, our contributions are as follows:

- We systematically extend traditional Instruction-Based Image Editing (IIE) to Hypothetical Instruction-Reasoning Image Editing (HI-IE). This task involves implicit, ambiguous, and

hypothetical editing instructions that demand deeper reasoning over contextual cues, physical dynamics, and user intent.

- We curate a new large-scale dataset, **Reason50K**, specifically designed to support the reasoning of hypothetical instruction in image editing. It contains 51,039 triplets of source image, hypothetical instruction, and target image, covering four distinct reasoning categories: physical, temporal, causal, and story-based reasoning.
- We propose **ReasonBrain**, a novel image editing framework that combines a MLLM with fine-grained reasoning cues extraction and a cross-modal enhancer. Together, these components endow the model with implicit cross-modal reasoning capabilities, enabling it to infer plausible, knowledge-grounded transformations and produce semantically coherent guidance for diffusion-based image editing under complex hypothetical scenarios.
- We conduct extensive experiments on both Reason50K and widely used benchmark datasets, demonstrating the effectiveness and generalization ability of ReasonBrain across reasoning-intensive and standard understanding-based editing scenarios.

## 2 Related Work

**Instruction-based Image Editing (IIE).** IIE [5] aims to train generative models to manipulate a given image based on user-provided instructions. A milestone in this field is InstructPix2Pix (IP2P) [5], which was the first to incorporate natural language instructions into image editing by fine-tuning a text-to-image (T2I) diffusion model on paired image-instruction datasets. Subsequent works have built upon IP2P by introducing novel curated datasets to enhance real-world editing performance and generate high-quality outputs [48, 18, 51, 26, 47]. Others have focused on improving instruction-output alignment by incorporating advanced techniques such as reward learning [50, 4] and multi-task training [38]. Recently, researchers have begun to integrate multimodal large language models (MLLMs) [43, 27] into existing image editing paradigms to enhance the model’s ability to understand complex instructions. We refer to these approaches as MLLM-enhanced methods [7, 17, 23, 45, 52, 42]. For instance, MGIE [7] leverages MLLMs to generate expressive instructions and provide explicit guidance, thereby enhancing editing performance. SmartEdit [17] further introduces a bidirectional interaction module that facilitates mutual understanding between the MLLM output and the input image. Despite recent advances, most existing efforts still rely on direct and explicit instructions (e.g., “Remove the ice”), limiting their ability to handle hypothetical instructions (e.g., “What would happen if the ice cube melted?”) that require deeper reasoning. While MLLMs offer general world knowledge, current frameworks lack mechanisms to extract and utilize fine-grained reasoning details. Our **ReasonBrain** builds upon the MLLM-enhanced paradigm by introducing dedicated reasoning-aware modules for generating precise visual guidance, with an emphasis on accurately inferring the implicit intent and real-world context embedded in hypothetical instructions.

**Reasoning-aware Datasets for Image Editing.** To date, only a few works have explored reasoning-aware datasets for image editing [17, 46, 19]. For instance, ReasonEdit [17] was designed primarily for evaluating the reasoning capabilities of image editing models and contains only a small set of textual samples, making it insufficient for training. Moreover, it focuses on object-level reasoning based on explicit instructions, while overlooking reasoning about editing operations themselves. EditWorld [46] aims to inject physical dynamics simulation capabilities into models across both realistic and virtual scenarios, but does not emphasize instruction-level reasoning. ReasonPix2Pix [19] introduces indirect instructions in a descriptive, goal-oriented style but lacks the depth and diversity needed for more advanced hypothetical reasoning. In contrast to these prior efforts, we curate **Reason50K**, a large-scale dataset specifically tailored for hypothetical instruction reasoning, enabling models to understand and execute complex edits grounded in physical, temporal, causal, and narrative scenarios.

## 3 Methodology

The goal of our work is to perform image editing by reasoning from a user-provided *hypothetical instruction*—an implicit, often ambiguous prompt that requires the model to infer the intended transformation through deeper reasoning about real-world context, physical dynamics, or potential outcomes (e.g., “What would happen if the sun were setting?”). We refer to this task as **Hypothetical Instruction-Reasoning Image Editing (HI-IE)**. To this end, we propose a unified solution

comprising a large-scale dataset, **Reason50K**, specifically curated to support the challenging task of hypothetical HI-IE, and a reasoning-aware image editing framework, **ReasonBrain**.

### 3.1 Reason50K for Reasoning Injecting

To support our proposed HI-IE task, we construct a novel large-scale dataset Reason50K specifically curated to inject *hypothetical instruction-reasoning ability* into image editing models. Reason50K contains 51,039 samples, each consisting of an input image, a corresponding hypothetical instruction, and a target edited image. Unlike existing datasets that primarily feature explicit or goal-oriented prompts (e.g., “Remove the animal in the mirror” or “Make it snowy”), our instructions are implicit, open-ended, and reasoning-driven (e.g., “What would happen if the ice cube were left at room temperature?” or “What would this bouquet look like if it were split into two separate rose bouquets?”). This shift introduces a significantly higher level of abstraction and demands real-world understanding. Reason50K is constructed using an inverse-style strategy, where the source image is generated from the target. Specifically, we leverage GPT [1] to produce hypothetical instructions based on user-provided prompts, and employ a diffusion model to generate multiple candidate source images. A hybrid scoring and evaluation scheme is then applied to select the most appropriate image, forming the final image pairs. Due to space limitations, the full data curation process is detailed in Appendix A. Moreover, Reason50K is organized around four distinct reasoning scenarios: **Physical Reasoning**, **Temporal Reasoning**, **Causal Reasoning**, and **Story Reasoning**, each illustrated with representative examples and instructions in Fig. 2.



Figure 2: Reasoning scenarios in Reason50K. The percentages in parentheses indicate the proportion of each category. The text below each sample shows an instruction of the corresponding reasoning type.

Table 1: Comparison of different datasets. Note that since ReasonPix2Pix [19] is not publicly available, we reference sample cases from their paper and exclude it from further experimental comparison (see Fig. 5).

Datasets	Reasoning Instruction	Automatic Generated	Open Domain	#Edits	#Editing Types	Source Example	Instruction	Target Example
ReasonPix2Pix [19]	✓	✓	✗	40,212	–		A colorful insect has landed	
EditWorld [46]	✗	✓	✓	8,674	7		Shifted her gaze to the left.	
ReasonEdit [17]	✗	✓	✗	219	–		Please remove the empty plate.	
Reason50K (Ours)	✓	✓	✓	51,039	4		What would happen if the cat stood in front of a mirror?	

**Reason50K vs. Existing Datasets.** Tab. 1 summarizes the key differences between our dataset and existing ones. In comparison: 1) *ReasonPix2Pix* [19] enhances instruction reasoning by using LLMs to rewrite explicit editing commands into goal-oriented implicit instructions. However, the dataset primarily consists of descriptive instructions and lacks more complex, abstract hypothetical instructions that require deeper contextual and causal reasoning. In addition, it lacks systematic categorization. 2) *EditWorld* [46] focuses on simulating world dynamics across both real and virtual scenarios. Although it includes some hypothetical instructions, its primary objective is to inject physical and temporal simulation capabilities into image editing models, rather than equipping them with implicit reasoning skills for understanding hypothetical instructions. Additionally, the overall scale of the EditWorld dataset is significantly smaller than ours. 3) *ReasonEdit* [17] is a small-scale dataset

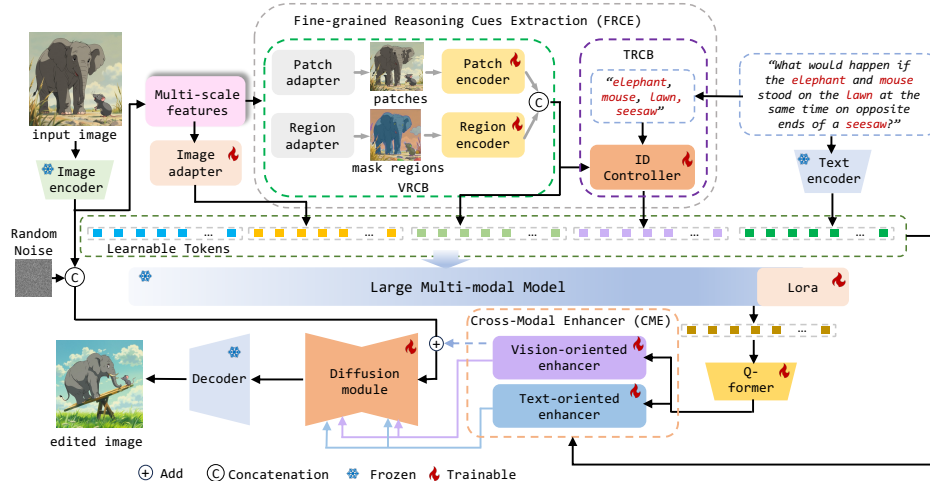


Figure 3: The overall framework of ReasonBrain. Given an input image  $I$  and a hypothetical instruction  $H$ , ReasonBrain first encodes them into multi-scale visual features and textual tokens using the image encoder  $\mathcal{E}_I(\cdot)$  and text encoder  $\mathcal{E}_T(\cdot)$ , respectively. These features are then passed into the FRCE module to learn detailed reasoning cues. Subsequently, all learned features are fed into the MLLM to generate visual guidance, which is further transformed via a QFormer to align with the diffusion model’s latent space. Finally, the resulting visual guidance interacts with the previously extracted fine-grained cues through a CME module to enhance semantic representation, which is then used to condition the diffusion model for final image generation.

designed primarily for evaluation. It focuses on object-level reasoning from explicit instructions and lacks both diversity and editing operation reasoning. Most importantly, it is not sufficient for model training. In contrast, our **Reason50K** is the first to provide *systematic, large-scale support* for training and evaluating *hypothetical instruction reasoning across diverse scenarios*. Each instruction requires deep reasoning grounded in contextual understanding and world knowledge—spanning physical, causal, temporal, and story-based scenarios—to guide image editing. This goes beyond surface-level transformations or explicit object manipulation. By incorporating carefully crafted hypothetical instructions, the dataset significantly promotes deeper semantic reasoning within image editing models.

### 3.2 ReasonBrain

ReasonBrain comprises an MLLM for visual guidance, reasoning, and a diffusion model responsible for conditional image generation. To support knowledge reasoning, we incorporate a Fine-Grained Reasoning Cues Extraction (FRCE) module. In addition, we introduce a Cross-Modal Enhancer (CME) to further enrich semantic representations through modality-specific refinement. The overall framework of ReasonBrain is illustrated in Fig. 3.

**Fine-grained Reasoning Cues Extraction.** Existing efforts utilize  $\mathcal{E}_I(I)$  and  $\mathcal{E}_T(H)$  directly for visual guidance generation, overlooking fine-grained cues critical for implicit reasoning, such as local object attributes, subtle spatial relationships, and context-dependent semantics between image regions and instructions, etc. To address this limitation, we introduce a Fine-Grained Reasoning Cues Extraction (FRCE) module, which comprises two specialized branches designed to capture fine-grained visual and textual reasoning cues, respectively.

(1) *Visual Reasoning Cues Branch (VRCB)*. This branch aims to extract fine-grained visual cues from both local and global perspectives. Specifically, the *local perspective* focuses on capturing object parts, textures, and spatial patterns, which are essential for implicit reasoning tasks involving fine object distinctions and subtle appearance changes. Inspired by the MAE framework [9], we first divide the visual features  $\mathcal{E}_I(I)$  into patches using a patch adapter  $\mathcal{P}(\cdot)$ , and then apply a patch-level feature extractor  $E_{\mathcal{P}}(\cdot)$  to obtain localized visual representations. This process is formalized as:  $R_{local} = E_{\mathcal{P}}(\mathcal{P}(\mathcal{E}_I(I)))$ . In contrast, the *global perspective* captures inter-object relationships and contextual information across the entire scene, which are beneficial for reasoning tasks that require an understanding of object interactions, event causality, and broader scene dynamics. We first employ an instance segmentation model (e.g., SAM [20, 34]) to segment objects from the background in

the image. Subsequently, a region-level feature extractor  $E_{\mathcal{R}}(\cdot)$  is trained to learn holistic semantic representations for each segmented instance. The entire process is formalized as:

$$R_{global} = E_{\mathcal{R}}(\text{SAM}(\mathcal{E}_I(I))). \quad (1)$$

After this dual-level operation, we concatenate  $R_{local}$  and  $R_{global}$  to form the final visual reasoning features  $R_V$  used for subsequent processing.

(2) *Textual Reasoning Cues Branch (TRCB)*. This branch aims to extract the key object referenced in  $H$ , serving as a bridge between linguistic intent and visual reasoning. Specifically, we first employ GPT [1] to extract the referenced object from the instruction and serialize it into a structured object token  $O$ . We then introduce an *ID Controller* to enhance the model’s ability to perform object-grounded reasoning by facilitating interaction between the object token and the visual reasoning features  $R_V$ . This module not only enriches the object token with visual context, enabling the model to reason about the object beyond its textual description, but also aligns the linguistic reference with its corresponding visual entity, helping to resolve ambiguities and prevent semantic drift during generation. The architecture of the ID Controller is illustrated in Fig. 4(a) and is implemented using a cross-attention layer [24] followed by a feed-forward network, formally defined as:

$$R_T = \text{FF}(\text{Cross-Atten}(R_V, O)). \quad (2)$$

Subsequently, following prior works [17, 52], we concatenate  $r$  additional learnable tokens  $\mathcal{Q} = \{[\text{IMG}_1], \dots, [\text{IMG}_r]\}$  with the extracted features and feed them into the MLLM for guidance generation. This operation transforms the implicit reasoning process into a token prediction task, where the MLLM learns to generate the embeddings of these  $r$  tokens, which serve as visual editing guidance. The process is formalized as:

$$\mathcal{T} = [\text{IA}(\mathcal{E}_I(I)), R_V, R_T, \mathcal{E}_T(H), \mathcal{Q}], \quad V = \text{MLLM}(\mathcal{T}; \theta). \quad (3)$$

Here,  $[\cdot, \cdot]$  denotes concatenation, and  $\text{IA}(\cdot)$  is a trainable image adapter that maps visual features into the MLLM’s latent space. The output  $V \in \mathbb{R}^{r \times d}$  represents the hidden embeddings of the  $r$  learnable tokens. In addition, we employ a QFormer [22] to align the feature space between the MLLM and the diffusion model, defined as  $\hat{V} = \text{QFormer}(V)$ .

**Cross-Modal Enhancer.** To compensate for the potential loss of visual and textual details in  $\hat{V}$ , we introduce a Cross-Modal Enhancer (CME). The CME consists of a *visual-oriented enhancer* and a *textual-oriented enhancer*, both implemented using the same bidirectional interaction mechanism. Specifically, each enhancer comprises five hybrid cross-attention blocks, followed by a linear projection layer and a normalization layer (see Fig. 4(b)). These modules reuse intermediate features generated both before and after the MLLM layer, enabling fine-grained semantic enhancement within each modality. Here, we illustrate the process using the visual-oriented enhancer. First, a set of learnable tokens  $Q^2$  interacts with  $\hat{V}$  (as key and value) via a cross-attention block to produce  $F_1$ . In parallel,  $\mathcal{E}_I(I)$  (query) attends to  $R_V$  in a second cross-attention block, yielding  $F_2$ . Next,  $F_1$  (query) and  $F_2$  (key and value) are fused via a third block, followed by a residual connection and normalization to obtain  $\bar{V}$ . This refined representation then serves as key and value in a fourth block, interacting with  $F_2$  (query). The output is further refined through a final cross-attention with  $R_V$ , producing the enhanced visual representation  $\bar{R}_V$ . Similarly, the textual-oriented enhancer is implemented by replacing  $\mathcal{E}_I(I)$  and  $R_V$  with  $\mathcal{E}_T(H)$  and  $R_T$ , respectively. Finally, the CME module outputs four enhanced features, which are passed to the diffusion model together with  $\mathcal{E}_I(I)$  and a noisy latent  $z$  for final image generation. Due to space limitations, the training objectives of ReasonBrain are provided in Appendix B.

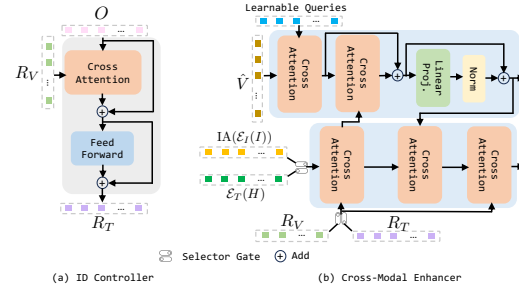


Figure 4: Network design of the (a) ID Controller and (b) Cross-Modal Enhancer.

<sup>2</sup>The newly introduced symbols are used only in this section to illustrate the visual-oriented enhancer.

## 4 Experiments

### 4.1 Setups: Datasets, Metrics, and Details

**Datasets:** We use Reason50K for both training and evaluation. Specifically, for each reasoning category, 400 samples are randomly selected for validation, while the remaining samples are used for training. In addition, we assess the reasoning capability of ReasonBrain on two external benchmarks: *ReasonEdit* [17] and *EditWorld* [46]. To evaluate generalization on conventional understanding scenarios, we further test on the *MagicBrush Test Set* [48] and the *Emu Edit Test Set* [38]. **Metrics:** To evaluate performance under reasoning scenarios, we adopt three metrics: *CLIP Score* [32], *MLLM Score* [46], and *Instruction Alignment (Ins-Align)* [17]. Specifically, we engage ten annotators to manually evaluate the outputs produced by different methods on the ReasonEdit++ dataset. The primary criterion is how well the edited image aligns with the given instruction. We then average the scores from all annotators to compute the final result. For understanding scenarios, we adopt *L1 distance*, *CLIP image similarity*, *DINO similarity*, *CLIP text-image similarity*, and *CLIP text-image direction similarity* as evaluation metrics. **Implementation Details:** During training, we adopt the pre-trained LLaVA v1.1-7B [27] and QFormer [22] and employ DeepSpeed [3] Zero-2 to perform LoRA [14] fine-tuning, with rank and alpha of 8 and 16, respectively. Following [17, 7], we expand the original LLM vocabulary with 32 new tokens, and the QFormer is composed of 6 transformer layers and 77 learnable query tokens. For the base editing model, we implement it with Flux [21] using FLUX.1-dev, which consists of 12B parameters. Models for other qualitative results are implemented using SD series [6, 39, 35, 2] with their original codebase. Our model is trained with a batch size of 16, and we use AdamW [28] optimizer to train the model with the weight decay as 1e-2 and the learning rate as 1e-3. All the experiments are conducted on 16 H20 GPUs. For a fair comparison, all baseline models are fine-tuned on the same training set used by ReasonBrain.

### 4.2 Quantitative Results

**Performance Comparison on Reasoning Scenarios.** The experimental results on Reason50K are summarized in Tab. 2, covering four distinct types of reasoning scenarios. ReasonBrain consistently outperforms all SOTA baselines across all metrics, demonstrating superior ability to infer hypothetical instructions and produce logically accurate edits aligned with world knowledge. While UltraEdit and PixWizard achieve competitive performance, their advantage mainly stems from exposure to massive datasets with diverse instructions rather than true reasoning capabilities. Notably, MLLM-enhanced methods such as MGIE and SmartEdit still underperform, indicating that simply integrating MLLMs or fine-tuning on reasoning datasets is insufficient without mechanisms for extracting fine-grained reasoning cues. These results further suggest that scaling data alone cannot bridge the reasoning gap without dedicated architectural modules and training objectives. Additionally, we select three representative methods for evaluation on ReasonEdit and EditWorld. As shown in Fig. 5, ReasonBrain, trained solely on our Reason50K, generalizes effectively to novel reasoning scenarios and achieves the best overall performance across datasets.

Table 2: Results on the Reason50K dataset for ReasonBrain and selected baselines. ↓ indicates that lower values are better, while ↑ indicates that higher values are better. The best results are highlighted in **bold**, and the second-best results are underlined.

Method	Physical Reasoning			Temporal Reasoning			Causal Reasoning			Story Reasoning			Total		
	CLIP↑	MLLM↑	Ins-Align↑	CLIP↑	MLLM↑	Ins-Align↑	CLIP↑	MLLM↑	Ins-Align↑	CLIP↑	MLLM↑	Ins-Align↑	CLIP↑	MLLM↑	Ins-Align↑
InstructPix2Pix [5]	0.083	0.825	0.211	0.207	0.846	0.678	0.153	0.785	0.191	0.196	0.628	0.225	0.160	0.771	0.326
MagicBrush [48]	0.102	0.844	0.335	0.228	0.877	0.725	0.162	0.802	0.344	0.209	0.635	0.359	0.175	0.790	0.441
MGIE [7]	0.098	0.802	0.288	0.213	0.832	0.685	0.155	0.761	0.328	0.201	0.622	0.322	0.167	0.754	0.406
SmartEdit [17]	0.118	0.849	<u>0.602</u>	0.226	0.881	0.779	0.165	0.823	0.385	<u>0.211</u>	0.655	0.361	0.180	0.802	0.532
UltraEdit [51]	0.156	0.861	0.584	0.231	0.922	0.826	<u>0.193</u>	<u>0.869</u>	<u>0.482</u>	0.209	0.669	<u>0.458</u>	<u>0.197</u>	0.830	<u>0.588</u>
PixWizard [25]	<u>0.161</u>	<u>0.881</u>	0.481	<u>0.234</u>	<u>0.951</u>	<u>0.833</u>	0.132	0.863	0.393	0.172	<u>0.697</u>	0.389	0.175	<u>0.848</u>	0.524
ReasonBrain (ours)	<b>0.186</b>	<b>0.902</b>	<b>0.846</b>	<b>0.267</b>	<b>0.977</b>	<b>0.894</b>	<b>0.282</b>	<b>0.891</b>	<b>0.858</b>	<b>0.301</b>	<b>0.736</b>	<b>0.798</b>	<b>0.259</b>	<b>0.877</b>	<b>0.847</b>

**Generalization Comparison on Understanding Scenarios.** As shown in Tab. 3, ReasonBrain achieves the best overall performance among all SOTA methods, demonstrating strong zero-shot generalization to new datasets. This result also highlights that, although trained solely on hypothetical instructions, ReasonBrain retains a robust understanding of clear, goal-directed editing commands. Furthermore, the competitive performance of Emu Edit, UltraEdit, and PixWizard suggests that scaling up with large and diverse datasets can further enhance model effectiveness on conventional instruction-based image editing tasks.

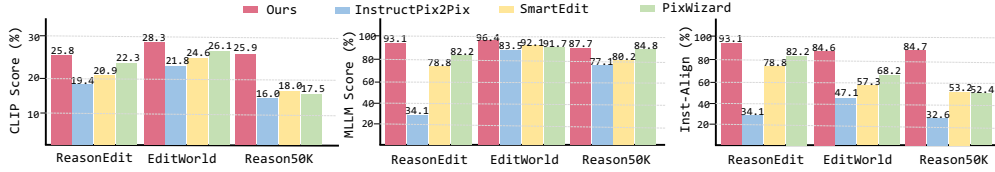


Figure 5: Results on ReasonEdit, EditWorld, and Reason50K for ReasonBrain and selected SOTA methods, highlighting performance under various reasoning datasets.

Table 3: Results on Emu Edit and MagicBrush test set for ReasonBrain and selected baselines.

Method	Emu Edit Test set					MagicBrush Test Set				
	CLIP <sub>dir</sub> ↑	CLIP <sub>im</sub> ↑	CLIP <sub>out</sub> ↑	L1↓	DINO↑	CLIP <sub>dir</sub> ↑	CLIP <sub>im</sub> ↑	CLIP <sub>out</sub> ↑	L1↓	DINO↑
InstructPix2Pix [5]	0.078	0.834	0.219	0.121	0.762	0.115	0.837	0.245	0.093	0.767
MagicBrush [48]	0.090	0.838	0.222	0.100	0.776	0.123	0.883	0.261	0.058	0.871
MGIE [7]	0.083	0.746	0.231	0.163	0.594	0.116	0.745	0.251	0.162	0.577
SmartEdit [17]	0.092	0.858	0.274	0.119	0.771	0.119	0.895	0.262	0.094	0.820
Emu Edit [38]	<u>0.109</u>	<u>0.859</u>	0.231	0.094	<u>0.819</u>	<u>0.135</u>	<u>0.897</u>	0.261	<u>0.052</u>	<u>0.879</u>
UltraEdit [51]	0.107	0.844	<u>0.283</u>	0.071	0.793	-	0.868	-	0.088	0.792
PixWizard [25]	0.104	0.845	<u>0.248</u>	<u>0.069</u>	0.798	0.124	<u>0.884</u>	<u>0.265</u>	0.063	0.876
ReasonBrain (ours)	<b>0.126</b>	<b>0.923</b>	<b>0.302</b>	<b>0.051</b>	<b>0.898</b>	<b>0.139</b>	<b>0.928</b>	<b>0.281</b>	<b>0.049</b>	<b>0.893</b>

### 4.3 Qualitative Results

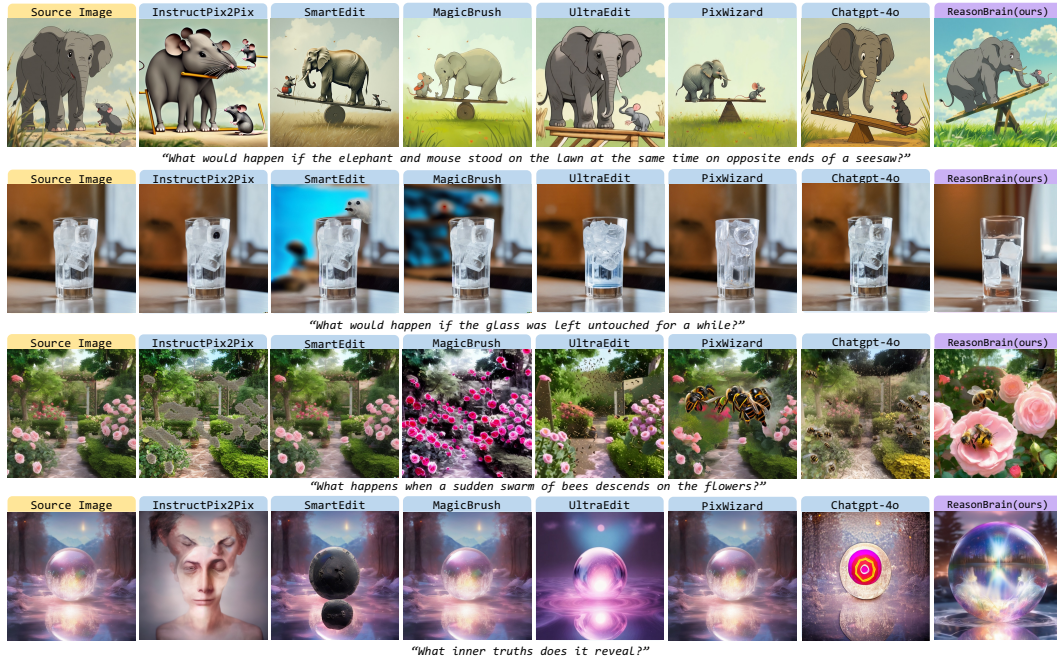


Figure 6: Qualitative comparison on Reason50K between ReasonBrain and selected SOTA methods. Compared to other SOTA methods, ReasonBrain demonstrates a strong ability to reason over implicit hypothetical instructions and produce semantically plausible edits grounded in world knowledge. As shown in Fig. 6, we visualize editing results of ReasonBrain and selected SOTA methods across four different reasoning scenarios. Our method demonstrates superior capability in executing hypothetical editing instructions by accurately reasoning about user intent, affected objects, and their plausible state transitions, while also maintaining stability in non-edited regions. For instance, in the first row (physical reasoning), our method successfully generates a physically plausible and contextually coherent scene—depicting the elephant and mouse standing on opposite ends of a seesaw, where the heavier elephant naturally tilts the seesaw downward. This highlights our model’s ability to reason about relative weight, spatial arrangement, and physical dynamics implied by the instruction. In contrast, InstructPix2Pix fails to capture the core intent, producing an irrelevant result. Other methods may include the correct objects mentioned in the instruction—such as the elephant,

mouse, and seesaw—but fall short in modeling their physical interactions, resulting in unrealistic or semantically inconsistent compositions. Notably, ChatGPT-4o produces an implausible outcome in which the mouse outweighs the elephant, contradicting basic physical intuition. We attribute this failure to hallucinations introduced by the language model [16].

#### 4.4 Ablation and Analysis

Table 4: Results of the ablation study on each component of ReasonBrain.

	with Patch Branch	with Region Branch	with ID Controller	with Vision Enhancer	with Text Enhancer	CLIP Score ↑	MLLM Score ↑	Ins-Align Score ↑
ReasonBrain	×	×	×	×	×	0.163	0.752	0.388
	✓	×	×	×	×	0.187	0.786	0.466
	✓	✓	×	×	×	0.206	0.802	0.529
	✓	✓	✓	×	×	0.239	0.833	0.758
	✓	✓	✓	✓	×	0.251	0.865	0.822
	✓	✓	✓	✓	✓	<b>0.259</b>	<b>0.877</b>	<b>0.847</b>

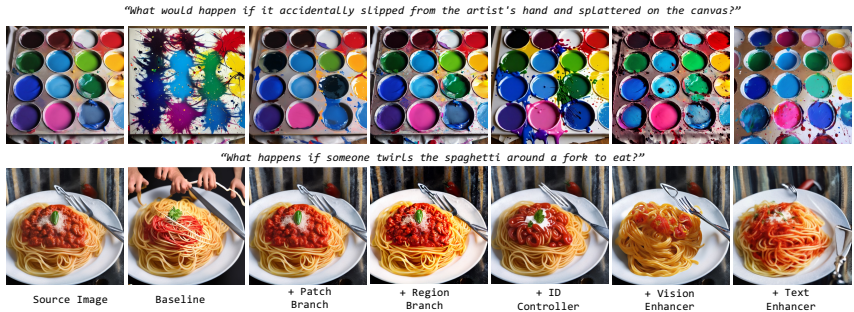


Figure 7: Qualitative comparison of ablation variants in ReasonBrain.

**Effectiveness of ReasonBrain’s Components.** To evaluate the contribution of each component in ReasonBrain, we conduct ablation experiments by progressively integrating key modules. As shown in Tab. 4 and Fig. 7, the fine-grained visual features help the model capture subtle visual cues essential for reasoning. The ID Controller significantly improves performance by preserving object identity during cross-modal alignment, which is critical for accurate instruction reasoning. Additionally, the CME module enhances overall generation quality by reinforcing modality-specific semantics and providing more detailed guidance.

**Impact of Each Visual Branch in VRCB.** As shown in Fig. 8, we visualize the individual and combined contributions of the patch and region branches in our VRCB. The patch branch captures local details such as texture variations and appearance changes, which are useful for modeling subtle transformations (e.g., wind effects on kite fabric or shifting crop colors). In contrast, the region branch focuses on global semantic structures and object-level understanding, such as the overall layout of the kite or the boundary of the burning field. When used independently, each branch captures only partial aspects of the intended edit. The patch branch may introduce local distortions without preserving object integrity, while the region branch may lack detailed variation. Their combination enables complementary integration of local precision and global semantics, resulting in more coherent, semantically accurate, and visually plausible edits under hypothetical instructions.

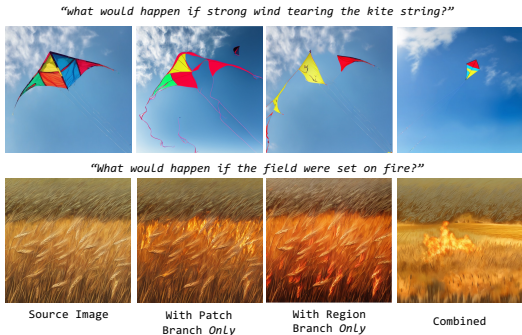


Figure 8: Qualitative comparison of patch and region branches in VRCB.

## 5 Conclusion

We extend instruction-based image editing to a hypothetical instruction reasoning setting and propose a unified solution from both dataset and model perspectives. Specifically, we curate Reason50K, a

large-scale dataset of 51,039 samples specifically designed to support hypothetical instruction reasoning across four diverse categories: physical, temporal, causal, and story reasoning. Simultaneously, we introduce ReasonBrain, a novel framework that enhances instruction reasoning by combining a MLLM and a fine-grained feature extraction module. We further integrate a cross-modal enhancer to enrich the semantics of the guidance used for diffusion-based editing. We conduct extensive experiments on both reasoning-intensive and conventional understanding scenarios, demonstrating that ReasonBrain exhibits strong reasoning capabilities as well as robust generalization performance. In addition, our Reason50K can facilitates broader advancements in reasoning-aware image generation, providing an extensible resource for future research in this emerging direction.

## References

- [1] J. Achiam, S. Adler, S. Agarwal, L. Ahmad, I. Akkaya, F. L. Aleman, D. Almeida, J. Altenschmidt, S. Altman, S. Anadkat, et al. Gpt-4 technical report. *arXiv preprint arXiv:2303.08774*, 2023.
- [2] S. AI. Stable diffusion 2.1 base. <https://huggingface.co/stabilityai/stable-diffusion-2-1-base>, 2022. Accessed: March 5, 2025.
- [3] R. Y. Aminabadi, S. Rajbhandari, A. A. Awan, C. Li, D. Li, E. Zheng, O. Ruwase, S. Smith, M. Zhang, J. Rasley, et al. Deepspeed-inference: enabling efficient inference of transformer models at unprecedented scale. In *SC22: International Conference for High Performance Computing, Networking, Storage and Analysis*, pages 1–15. IEEE, 2022.
- [4] J. Bai, W. Chow, L. Yang, X. Li, J. Li, H. Zhang, and S. Yan. Humanedit: A high-quality human-rewarded dataset for instruction-based image editing. *arXiv preprint arXiv:2412.04280*, 2024.
- [5] T. Brooks, A. Holynski, and A. A. Efros. Instructpix2pix: Learning to follow image editing instructions. In *Proceedings of the IEEE/CVF conference on computer vision and pattern recognition*, pages 18392–18402, 2023.
- [6] CompVis. Stable diffusion v1.4. <https://huggingface.co/CompVis/stable-diffusion-v1-4>, 2022. Accessed: March 5, 2025.
- [7] T.-J. Fu, W. Hu, X. Du, W. Y. Wang, Y. Yang, and Z. Gan. Guiding Instruction-based Image Editing via Multimodal Large Language Models. In *International Conference on Learning Representations (ICLR)*, 2024.
- [8] Z. Geng, B. Yang, T. Hang, C. Li, S. Gu, T. Zhang, J. Bao, Z. Zhang, H. Li, H. Hu, et al. Instructdiffusion: A generalist modeling interface for vision tasks. In *Proceedings of the IEEE/CVF Conference on computer vision and pattern recognition*, pages 12709–12720, 2024.
- [9] K. He, X. Chen, S. Xie, Y. Li, P. Dollár, and R. Girshick. Masked autoencoders are scalable vision learners. In *Proceedings of the IEEE/CVF conference on computer vision and pattern recognition*, pages 16000–16009, 2022.
- [10] Q. He, J. Peng, P. Xu, B. Jiang, X. Hu, D. Luo, Y. Liu, Y. Wang, C. Wang, X. Li, et al. Dynamiccontrol: Adaptive condition selection for improved text-to-image generation. *arXiv preprint arXiv:2412.03255*, 2024.
- [11] S. He, A. Ming, Y. Li, J. Sun, S. Zheng, and H. Ma. Thinking image color aesthetics assessment: Models, datasets and benchmarks. In *Proceedings of the IEEE/CVF International Conference on Computer Vision*, pages 21838–21847, 2023.
- [12] J. Ho, A. Jain, and P. Abbeel. Denoising diffusion probabilistic models. *Advances in neural information processing systems*, 33:6840–6851, 2020.
- [13] A. Hore and D. Ziou. Image quality metrics: Psnr vs. ssim. In *2010 20th international conference on pattern recognition*, pages 2366–2369. IEEE, 2010.
- [14] E. J. Hu, Y. Shen, P. Wallis, Z. Allen-Zhu, Y. Li, S. Wang, L. Wang, and W. Chen. Lora: Low-rank adaptation of large language models. *arXiv preprint arXiv:2106.09685*, 2021.

- [15] E. J. Hu, Y. Shen, P. Wallis, Z. Allen-Zhu, Y. Li, S. Wang, L. Wang, W. Chen, et al. Lora: Low-rank adaptation of large language models. *ICLR*, 1(2):3, 2022.
- [16] L. Huang, W. Yu, W. Ma, W. Zhong, Z. Feng, H. Wang, Q. Chen, W. Peng, X. Feng, B. Qin, and T. Liu. A survey on hallucination in large language models: Principles, taxonomy, challenges, and open questions. *ACM Trans. Inf. Syst.*, 43(2), Jan. 2025. ISSN 1046-8188. doi: 10.1145/3703155. URL <https://doi.org/10.1145/3703155>.
- [17] Y. Huang, L. Xie, X. Wang, Z. Yuan, X. Cun, Y. Ge, J. Zhou, C. Dong, R. Huang, R. Zhang, et al. Smartedit: Exploring complex instruction-based image editing with multimodal large language models. In *Proceedings of the IEEE/CVF Conference on Computer Vision and Pattern Recognition*, pages 8362–8371, 2024.
- [18] M. Hui, S. Yang, B. Zhao, Y. Shi, H. Wang, P. Wang, Y. Zhou, and C. Xie. Hq-edit: A high-quality dataset for instruction-based image editing. *arXiv preprint arXiv:2404.09990*, 2024.
- [19] Y. Jin, P. Ling, X. Dong, P. Zhang, J. Wang, and D. Lin. Reasonpix2pix: instruction reasoning dataset for advanced image editing. *arXiv preprint arXiv:2405.11190*, 2024.
- [20] A. Kirillov, E. Mintun, N. Ravi, H. Mao, C. Rolland, L. Gustafson, T. Xiao, S. Whitehead, A. C. Berg, W.-Y. Lo, P. Dollár, and R. Girshick. Segment anything. *arXiv:2304.02643*, 2023.
- [21] B. F. Labs. Flux. <https://github.com/black-forest-labs/flux>, 2024.
- [22] J. Li, D. Li, S. Savarese, and S. Hoi. Blip-2: Bootstrapping language-image pre-training with frozen image encoders and large language models. In *International conference on machine learning*, pages 19730–19742. PMLR, 2023.
- [23] Y. Li, Y. Bian, X. Ju, Z. Zhang, Y. Shan, Y. Zou, and Q. Xu. Brushedit: All-in-one image inpainting and editing. *arXiv preprint arXiv:2412.10316*, 2024.
- [24] H. Lin, X. Cheng, X. Wu, and D. Shen. CAT: Cross Attention in Vision Transformer . In *2022 IEEE International Conference on Multimedia and Expo (ICME)*, pages 1–6, 2022.
- [25] W. Lin, X. Wei, R. Zhang, L. Zhuo, S. Zhao, S. Huang, H. Teng, J. Xie, Y. Qiao, P. Gao, et al. Pixwizard: Versatile image-to-image visual assistant with open-language instructions. *arXiv preprint arXiv:2409.15278*, 2024.
- [26] C. Liu, X. Li, and H. Ding. Referring image editing: Object-level image editing via referring expressions. In *Proceedings of the IEEE/CVF Conference on Computer Vision and Pattern Recognition*, pages 13128–13138, 2024.
- [27] H. Liu, C. Li, Q. Wu, and Y. J. Lee. Visual instruction tuning. *Advances in neural information processing systems*, 36, 2024.
- [28] I. Loshchilov and F. Hutter. Decoupled weight decay regularization. *arXiv preprint arXiv:1711.05101*, 2017.
- [29] F. Meng, W. Shao, L. Luo, Y. Wang, Y. Chen, Q. Lu, Y. Yang, T. Yang, K. Zhang, Y. Qiao, et al. Phybench: A physical commonsense benchmark for evaluating text-to-image models. *arXiv preprint arXiv:2406.11802*, 2024.
- [30] T.-T. Nguyen, D.-A. Nguyen, A. Tran, and C. Pham. Flexedit: Flexible and controllable diffusion-based object-centric image editing. *arXiv preprint arXiv:2403.18605*, 2024.
- [31] T. T. Nguyen, Z. Ren, T. Pham, T. T. Huynh, P. L. Nguyen, H. Yin, and Q. V. H. Nguyen. Instruction-guided editing controls for images and multimedia: A survey in llm era. *arXiv preprint arXiv:2411.09955*, 2024.
- [32] A. Radford, J. W. Kim, C. Hallacy, A. Ramesh, G. Goh, S. Agarwal, G. Sastry, A. Askell, P. Mishkin, J. Clark, et al. Learning transferable visual models from natural language supervision. In *International conference on machine learning*, pages 8748–8763. PmLR, 2021.

- [33] A. Ramesh, P. Dhariwal, A. Nichol, C. Chu, and M. Chen. Hierarchical text-conditional image generation with clip latents. *arXiv preprint arXiv:2204.06125*, 1(2):3, 2022.
- [34] N. Ravi, V. Gabeur, Y.-T. Hu, R. Hu, C. Ryali, T. Ma, H. Khedr, R. Rädle, C. Rolland, L. Gustafson, et al. Sam 2: Segment anything in images and videos. *arXiv preprint arXiv:2408.00714*, 2024.
- [35] R. Rombach, A. Blattmann, D. Lorenz, P. Esser, and B. Ommer. High-resolution image synthesis with latent diffusion models. In *Proceedings of the IEEE/CVF Conference on Computer Vision and Pattern Recognition (CVPR)*, pages 10684–10695, June 2022.
- [36] R. Rombach, A. Blattmann, D. Lorenz, P. Esser, and B. Ommer. High-resolution image synthesis with latent diffusion models. In *Proceedings of the IEEE/CVF conference on computer vision and pattern recognition*, pages 10684–10695, 2022.
- [37] C. Saharia, W. Chan, S. Saxena, L. Li, J. Whang, E. L. Denton, K. Ghasemipour, R. Gontijo Lopes, B. Karagol Ayan, T. Salimans, et al. Photorealistic text-to-image diffusion models with deep language understanding. *Advances in neural information processing systems*, 35: 36479–36494, 2022.
- [38] S. Sheynin, A. Polyak, U. Singer, Y. Kirstain, A. Zohar, O. Ashual, D. Parikh, and Y. Taigman. Emu edit: Precise image editing via recognition and generation tasks. In *Proceedings of the IEEE/CVF Conference on Computer Vision and Pattern Recognition*, pages 8871–8879, 2024.
- [39] SimianLuo. Lcm dreamshaper v7. [https://huggingface.co/SimianLuo/LCM\\_Dreamshaper\\_v7](https://huggingface.co/SimianLuo/LCM_Dreamshaper_v7), 2024. Accessed: March 5, 2025.
- [40] J. Sohl-Dickstein, E. Weiss, N. Maheswaranathan, and S. Ganguli. Deep unsupervised learning using nonequilibrium thermodynamics. In *International conference on machine learning*, pages 2256–2265. pmlr, 2015.
- [41] Q. Sun, J. Luo, D. Zhang, and X. Li. Smartfreedit: Mask-free spatial-aware image editing with complex instruction understanding. *arXiv preprint arXiv:2504.12704*, 2025.
- [42] X. Tian, W. Li, B. Xu, Y. Yuan, Y. Wang, and H. Shen. Mige: A unified framework for multimodal instruction-based image generation and editing. *arXiv preprint arXiv:2502.21291*, 2025.
- [43] H. Touvron, T. Lavril, G. Izacard, X. Martinet, M.-A. Lachaux, T. Lacroix, B. Rozière, N. Goyal, E. Hambro, F. Azhar, et al. Llama: Open and efficient foundation language models. *arXiv preprint arXiv:2302.13971*, 2023.
- [44] Y. Wang, W. Chen, X. Han, X. Lin, H. Zhao, Y. Liu, B. Zhai, J. Yuan, Q. You, and H. Yang. Exploring the reasoning abilities of multimodal large language models (mllms): A comprehensive survey on emerging trends in multimodal reasoning. *arXiv preprint arXiv:2401.06805*, 2024.
- [45] Z. Wang, A. Li, Z. Li, and X. Liu. Genartist: Multimodal llm as an agent for unified image generation and editing. *Advances in Neural Information Processing Systems*, 37:128374–128395, 2024.
- [46] L. Yang, B. Zeng, J. Liu, H. Li, M. Xu, W. Zhang, and S. Yan. Editworld: Simulating world dynamics for instruction-following image editing. *arXiv preprint arXiv:2405.14785*, 2024.
- [47] Q. Yu, W. Chow, Z. Yue, K. Pan, Y. Wu, X. Wan, J. Li, S. Tang, H. Zhang, and Y. Zhuang. Anyedit: Mastering unified high-quality image editing for any idea. *arXiv preprint arXiv:2411.15738*, 2024.
- [48] K. Zhang, L. Mo, W. Chen, H. Sun, and Y. Su. Magicbrush: A manually annotated dataset for instruction-guided image editing. *Advances in Neural Information Processing Systems*, 36: 31428–31449, 2023.
- [49] R. Zhang, P. Isola, A. A. Efros, E. Shechtman, and O. Wang. The unreasonable effectiveness of deep features as a perceptual metric. In *Proceedings of the IEEE conference on computer vision and pattern recognition*, pages 586–595, 2018.

- [50] S. Zhang, X. Yang, Y. Feng, C. Qin, C.-C. Chen, N. Yu, Z. Chen, H. Wang, S. Savarese, S. Ermon, et al. Hive: Harnessing human feedback for instructional visual editing. In *Proceedings of the IEEE/CVF Conference on Computer Vision and Pattern Recognition*, pages 9026–9036, 2024.
- [51] H. Zhao, X. S. Ma, L. Chen, S. Si, R. Wu, K. An, P. Yu, M. Zhang, Q. Li, and B. Chang. Ultraedit: Instruction-based fine-grained image editing at scale. *Advances in Neural Information Processing Systems*, 37:3058–3093, 2024.
- [52] J. Zhou, J. Li, Z. Xu, H. Li, Y. Cheng, F.-T. Hong, Q. Lin, Q. Lu, and X. Liang. Fireedit: Fine-grained instruction-based image editing via region-aware vision language model. *arXiv preprint arXiv:2503.19839*, 2025.

## Appendix

### A Dataset Generation

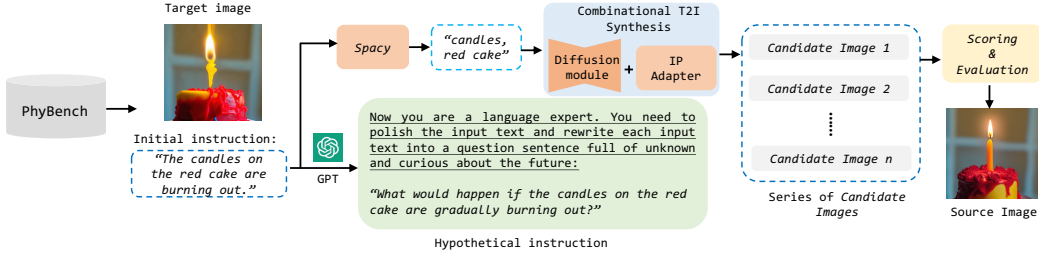


Figure A1: Data generation process.

The construction of our data consists of two parts. The first part (over 90% of the entire dataset) is generated following the pipeline illustrated in Fig. A1, which adopts an inverse generation strategy—deriving the source image from the target. Specifically, we first adopt the same procedure as PhyBench [29] to generate target images along with their initial instructions. Each initial instruction is then rewritten into a hypothetical form using prompt-based rewriting with GPT [1]. In parallel, we use SpaCy<sup>3</sup> to perform named entity recognition (NER) on the initial instruction to extract candidate objects for source image generation. These candidates are passed to a diffusion model equipped with an IP-Adapter to synthesize multiple image variants. Each candidate image is subsequently evaluated by GPT, and the top-N images are selected based on a combination of GPT scores and perceptual quality metrics [11, 13, 49]. Each selected image, along with the corresponding hypothetical instruction and target image, constitutes a sample in our dataset. The second part (less than 10%) consists of story-type samples derived from EditWorld [46]. We apply the same instruction rewriting, scoring, and filtering process to refine and select high-quality samples for inclusion.

### B Training Objectives of ReasonBrain

The training of ReasonBrain comprises two components: fine-tuning the MLLM and optimizing the diffusion model. Specifically, for fine-tuning the MLLM, we freeze most of its parameters and apply Low-Rank Adaptation (LoRA) [15] for efficient adaptation. The objective is defined as:

$$\mathcal{L}_{MLLM} = - \sum_{i=1}^T \log p_{\{\theta \cup \theta_{LoRA}\}}([\text{IMG}_i] \mid \text{IA}(\mathcal{E}_I(I)), R_V, R_T, \mathcal{E}_T(H), [\text{IMG}_1], \dots, [\text{IMG}_{i-1}]), \quad (\text{A1})$$

where  $\theta_{LoRA}$  denotes the trainable parameters introduced by LoRA. This loss minimizes the negative log-likelihood of predicting each learnable token  $[\text{IMG}_i]$  conditioned on the fine-grained features and previously predicted tokens. For image generation, we adopt a latent diffusion objective:

$$\mathcal{L}_{DM} = \mathbb{E}_{\mathcal{E}_I(I), \mathcal{E}_I(I), H, \epsilon, t} \left[ \left\| \epsilon - \epsilon_{\delta}(t, [z_t, \mathcal{E}_I(I)] + \bar{R}_{visual} + \bar{R}_{text}, [\bar{e}_{visual}, \bar{e}_{text}]) \right\|_2^2 \right], \quad (\text{A2})$$

where  $\epsilon \sim \mathcal{N}(0, 1)$  is the sampled noise and  $z_t$  is the noisy latent at timestep  $t$ .  $\epsilon_{\delta}(\cdot)$  denotes the denoising network trained to predict the added noise based on the timestep and the provided visual reasoning guidance. The overall training objective is defined as the sum of the MLLM and diffusion losses:  $\mathcal{L} = \mathcal{L}_{MLLM} + \mathcal{L}_{DM}$ .

### C More Qualitative Results

To further demonstrate the editing performance of ReasonBrain compared to SOTA methods, we present additional qualitative results in Fig. A2 and Fig. A3. It is evident that ReasonBrain consistently outperforms other SOTA approaches, producing more coherent and visually plausible edits. These results highlight ReasonBrain’s ability to reason effectively from hypothetical instructions and generate outputs that closely align with the transformations implied by the underlying reasoning.

<sup>3</sup><https://spacy.io/>

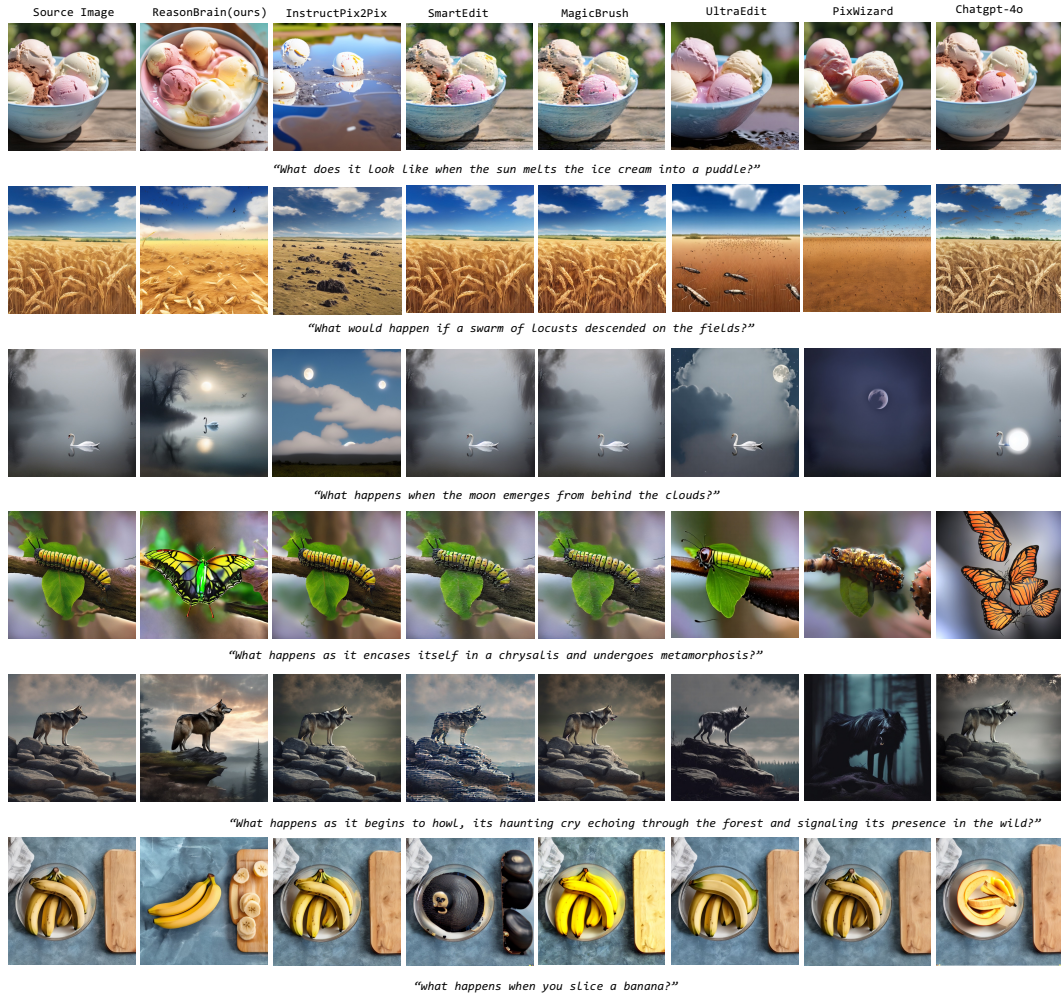


Figure A2: Qualitative comparison on Reason50K between ReasonBrain and selected SOTA methods.

## D Broader Impact and Ethics Statement

We plan to make the dataset and associated code publicly available for research. Nonetheless, we acknowledge the potential for misuse, particularly by those aiming to generate misinformation using our methodology. We will release our code under an open-source license with explicit stipulations to mitigate this risk.

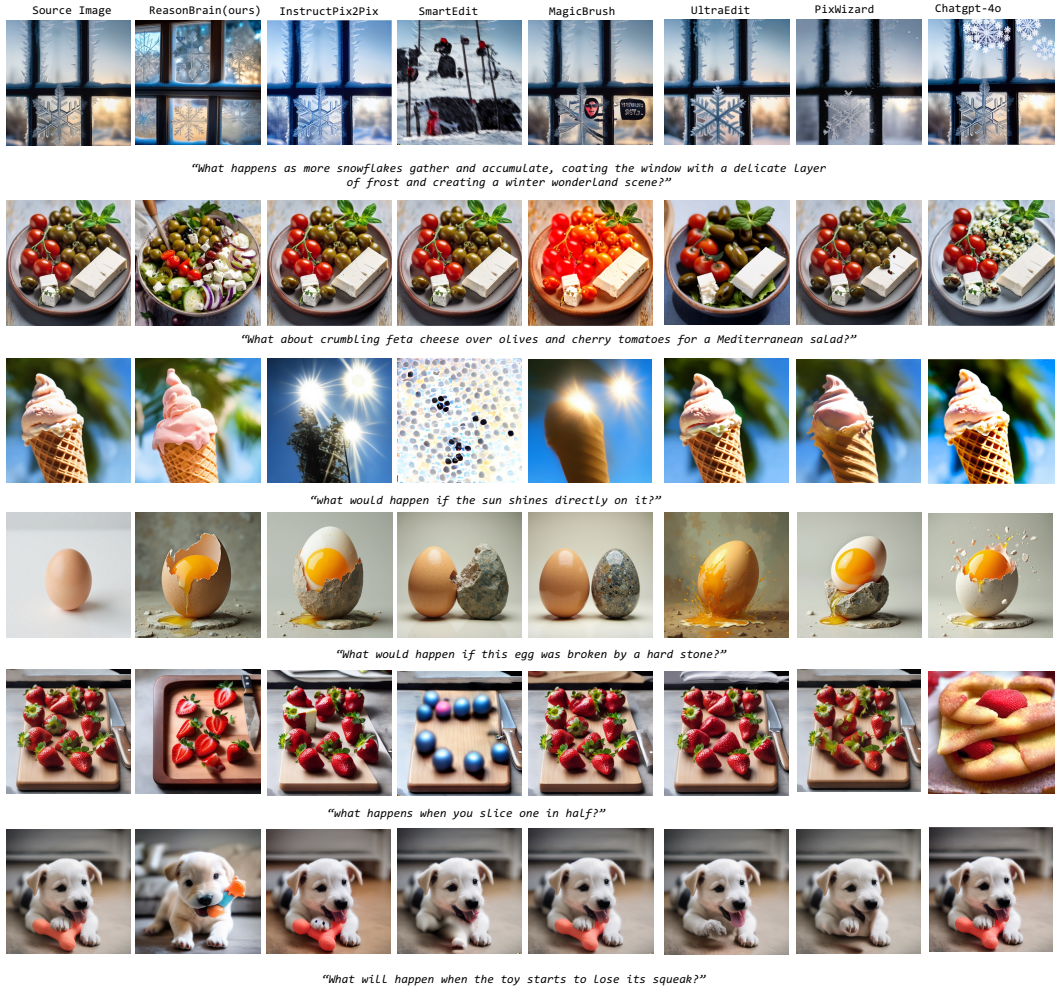


Figure A3: Qualitative comparison on Reason50K between ReasonBrain and selected SOTA methods.